AIAA JOURNAL
Vol. 57, No. 9, September 2019

Passive Pitching of a Flapping Wing in Turning Flight

Samane Zeyghami*
Lehigh University, Bethlehem, Pennsylvania 18015
Qiang Zhong†
University of Virginia, Charlottesville, Virginia 22903
Geng Liu‡
University of Maine, Orono, Maine 04468
and
Haibo Dong§
University of Virginia, Charlottesville, Virginia 22903

DOI: 10.2514/1.J056622

Insect wings are flexible structures that passively deform under the action of inertial and aerodynamic forces in flight. Previous studies have focused on the aerodynamic and energetic merits of these deformations. Here, the effect of torsional wing flexibility on maneuverability is investigated by modeling the dynamics of the wing pitch motion when body yaw rotation is imposed. Analyses were carried out for different nondimensional stiffness levels, characterized by Cauchy number and body-to-wing velocity ratios Ω/ω. In addition, the impacts of inertial effects were evaluated via changing mass ratio. It was demonstrated that body rotations change the balance between the aerodynamic and elastic torque exerted about the wings' pitching axes. This results in passive variations in the wing pitch angles that are bilaterally asymmetric and increase linearly with the ratio of the body rotational velocity to the wing flapping velocity $\bar{\Omega}$. The passive changes in the bilateral pitch angles induce a torque about the body's yaw rotation, which curtails rotational damping effects due to the flapping motion of the wings, known as flapping counter-torque. The results reveal that torsionally flexible wing designs could enhance maneuverability by mitigating the need for active wing kinematic modulations during aerial maneuvers.

Nomenclature

b	=	wing span, m
C_L	=	lift coefficient
C_T	=	thrust coefficient
Ch	=	Cauchy number
c	=	wing chord, m
I	=	wing moment of inertia
I_b	=	body moment of inertia
K	=	reduced frequency
M	=	mass ratio
Re	=	Reynolds number
U	=	wing-tip velocity, m/s
ΔA	=	bilateral difference in half-stroke-averaged value of any variable A
Ω	=	yaw velocity of the body, rad/s
ω	=	flapping velocity of the wing, rad/s

I. Introduction

EXPERIMENTAL observations and measurements have reported flexibility of insect wings with various deformation modes, including twisting, cambering, and spanwise bending [1–3]. Researchers have most commonly associated wing flexibility with enhancing the aerodynamic performance. It has been shown that the wing deformations are beneficial to improving force production capacity [4–6] and/or power economy [7,8]. Recent investigations have found other benefits associated with wing flexibility, such as reduction of collision damage [9] and detection of the body angular velocity via sensing the changes in the structural dynamics of the wing [10]. Overall, it appears that the effect of wing flexibility on insect flight is broader than its mere aerodynamic merits, and more studies need to be done to unravel its contribution to other aspects of flight.

Wings of insects are complex structures, consisting of a membrane and a network of tabular veins [11]. For many insects, there exists a high-torsional-flexibility region concentrated at the wing hinge [6,11], which directly affects the passive pitching motion of the wing during both translational phase of the flapping stroke and fast rotation at the stroke reversal [12,13]. The network of veins across the wing surface provides another means for enhancing the torsional flexibility of the wing, causing the wing surface to twist under the action of the inertial and aerodynamic forces acting on it. Measurements on free-flying insects have indicated that twisting can result in 10–30 deg difference between the pitch angles of the wing root and that of the wing tip [3,11,14]. Nevertheless, although twisting improves the aerodynamic efficiency, its contribution to the magnitude of the force is rather small [15]. Therefore, to probe how the passive deformations of the wing affect the aerodynamics as well as the performance of the insect flight, many computational studies modeled the combined effect of the flexibility of wing hinge and its surface as a lumped torsional spring located at the wing base [12,13,16–21].

Wing pitch angle and its dynamics play an important role in the aerodynamic force generation of flapping flight. For instance, insects flap their wings at high pitch angles through the air. This motion creates a vortex at the leading edge that remains attached to the wing, generating large unsteady aerodynamic forces [22]. In addition, fast wing flip at the stroke reversal enhances circulation on the wing, providing another mechanism for aerodynamic force generation [23,24]. Because of large sensitivity of both the magnitude and direction of aerodynamic force to wing pitching, many insects adjust this angle to steer and maneuver [8,17,18,25–28]. Previously, it was assumed that the control of the wing kinematics, including the wing pitch, is directly carried out by the flight muscles in the thorax. However, recent studies have suggested that the interactions of the flapping wing with its own unsteady flow should be considered when

Received 15 August 2017; revision received 4 January 2018; accepted for publication 15 January 2018; published online 12 February 2018.

*Postdoctoral Researcher, Department of Mechanical Engineering and Mechanics.
†Ph.D. Student, Mechanical and Aerospace Engineering.
‡Postdoctoral Researcher, Department of Mechanical Engineering; geng.liu@maine.edu. Member AIAA.
§Associate Professor, Mechanical and Aerospace Engineering.

studying the mechanics of the wing kinematics control in insects. For instance, investigations on the free flight of fruit flies have indicated that the torsional flexibility of the wing hinge allows these insects to indirectly control their wing pitch angles during aerial maneuvers [17,18].

When an insect is in hovering or low-speed flight, the motion of the bilateral wings is symmetric. However, any lateral motion (translation or rotation) is usually induced by asymmetrically varying the kinematics of the bilateral wings. Previous studies have suggested that these changes in the wing kinematics are enforced by an intricate chain of actions that is controlled by the insects' nervous system [29]. We refer to these changes as active wing kinematics variations. When an animal (voluntarily) begins turning, active generation of aerodynamic torque about the desired rotation axis is inevitable. This phase of motion is referred to as the acceleration phase, where body rotational velocity increases. However, decelerating and stopping may not be entirely active because the damping forces such as friction tend to inhibit the motion [30]. Particularly, a series of recent studies have suggested that the dynamics of the deceleration phase in slow aerial yaw turns are dominated by a passive aerodynamic torque generation mechanism: the so-called flapping counter-torque (FCT). They suggested that the difference in the net velocity of the bilateral wings, when the body is in yaw rotation about an axis normal to the plane of flapping, induces a damping torque, which acts as a breaking mechanism. This damping torque exists even if the motion of the bilateral wings is symmetric. For the simplified scenario where no active control is present, the magnitude of the damping torque is proportional to the magnitude of the body velocity, resulting in an exponential decay in the rate of body rotation. The predictions of this model were successfully confirmed by experimental measurements on slow yaw turns of several species of insects and birds. Nevertheless, more recent measurements on fast yaw turns of some agile insects such as dragonflies and damselflies [26,31,32] show that the FCT model alone is insufficient in explaining the dynamics of these fast aerial maneuvers.

To better understand the dynamics of fast aerial maneuvers of flying insects and to probe how the wing flexibility plays a role in enhancing maneuverability, Zeyghami and Dong [26] and Zeyghami [32] investigated the behavior of a pair of flexible flapping wings when they undergo yaw rotation. They employed a torsional spring at the wing's rotation axis as a first-order model of the wing's torsional flexibility and a quasi-steady model to estimate aerodynamic force and moment. They showed that the motion of the bilateral wings passively changes in response to the body motion. Here, we conduct a similar study in which we use an in-house high-fidelity computational fluid dynamics (CFD) tool to calculate the aerodynamic forces and to unravel the unsteady flow features of maneuvering flight. Similar to the aforementioned study, we model the wing's torsional flexibility via a torsional spring located close to the leading edge as a first-order approximation of the insect wing structure. We particularly seek to answer two questions. Does body rotation during aerial maneuvers affect the dynamics of wing pitch? And if so, how do the changes in wing motion influence the performance of aerial maneuvers?

II. Methods

A. Problem Definition

Here, we are interested only in the deceleration phase of the maneuver where the active manipulation of the wing kinematics is minimal [30,33]. Therefore, we assume that the flapping motion of the bilateral wings is symmetric. The pitching of the wing about its rotation axis, on the other hand, may not be symmetric because it is dictated by the combined effect of the aerodynamic, elastic, and inertial forces acting about the wing's rotation axis.

When the body is in rotation about an axis normal to the plane of flapping, in downstroke (DS), the net rotational velocity of the outer wing increases, and that of the inner wing decreases. The opposite occurs in upstroke (US), where the velocity of the inner wing increases, and that of the outer wing decreases. Thus, the behavior of the inner wing in DS is identical to that of the outer wing in US. The same can be said about the behavior of the inner wing in US and outer wing in DS. Thus, to simplify the computations, we only modeled one wing. The difference in the dynamics of the inner and outer wings can be obtained by analyzing DS and US of the outer wing only.

The wing is modeled as a thin cylinder with elliptical cross section. Figure 1 shows the schematic of the wing. Wing aspect ratio, defined as the ratio of the major to minor axis length of the ellipse, was kept constant. Flapping motion is defined as rotation about the y axis of the body-fixed coordinate system where the origin is set at the body's centerline $0.1c$ away from the wing root. The flapping profile is sinusoidal with constant amplitude of 100 deg.

The dynamics of the passive wing pitching is governed by the combined effect of the wing morphology, structure, wing and body kinematics, and flow properties. It is not immediately obvious if all these parameters have independent effects on the output. Dimensional analysis was performed to combine the effect of individual parameters in the form of physically relevant nondimensional quantities as listed follows (detailed derivation of the nondimensional numbers are carried out in [12]):

$$\eta = f\left(Ch, M, Re, K, \bar{\Omega}\right) \tag{1}$$

where η is the wing pitch angle, and $Ch = (\rho\Phi^2 f^2 c^3 b^2)/G$ is the nondimensional flexibility of the combined fluid–structure system and is defined as the ratio of the fluid dynamic pressure to the structure elastic forces. f, c, b, and Φ are the flapping frequency, chord, span, and flapping amplitude, respectively. G is the torsional stiffness of the spring. $M = \rho_s t/\rho c$ is the mass ratio, where ρ and ρ_s are the fluid and solid densities, and t is the wing thickness. $Re = \rho cU/\mu$, where $U = 2f\Phi b$ is the velocity of the wing tip. $K = fc/U$ is the reduced frequency. $\bar{\Omega} = \Omega/\omega$ is the normalized body velocity, defined as the ratio of the body yaw velocity Ω and wing flapping velocity $\omega = 2\Phi f$.

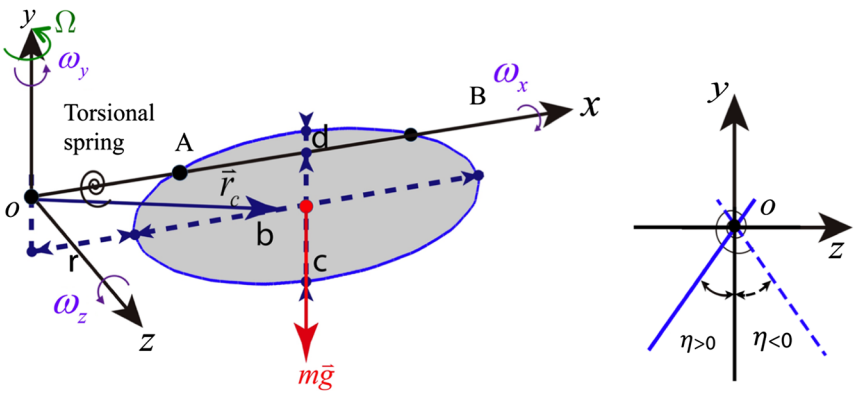

Fig. 1 Schematic of the model flapping wing in yaw rotation. Yaw angular velocity of the body is oriented in the positive y direction.

In all simulations, we kept Reynolds number constant at 500. Cauchy number, M, and $\bar{\Omega}$ are the inputs and vary among the simulations. For insects, $M \approx 1$ [34]. For aquatic animals, this ratio is closer to 0.1.

The output is the wing passive pitching motion as well as the resulting aerodynamic forces and moments. The half-stroke-averaged force coefficients are defined as follows:

$$C_T = \frac{\bar{T}}{0.5\rho b^3 c(\omega \pm \Omega)^2} \tag{2}$$

$$C_L = \frac{\bar{L}}{0.5\rho b^3 c(\omega \pm \Omega)^2} \tag{3}$$

where $\bar{T}$ and $\bar{L}$ are the average horizontal and vertical force in downstroke or upstroke, respectively. The fluid force is normalized by the net flapping velocity of the wing in the ground coordinate system (rather than the flapping velocity in the body-fixed coordinate). This is to separate the effect of the change in the net velocity of the wing in altering the fluid forces. For the outer wing, the net flapping velocity is $\omega + \Omega$ in downstroke (DS) and $\omega - \Omega$ in upstroke (US).

B. Numerical Modeling

The incompressible flow is governed by the three-dimensional Navier–Stokes equations, which can be written in tensor form as follows:

$$\frac{\partial u_i}{\partial x_i} = 0; \qquad \frac{\partial u_i}{\partial t} + \frac{\partial u_i u_j}{\partial x_j} = -\frac{\partial p}{\partial x_i} + \frac{1}{Re}\frac{\partial^2 u_i}{\partial x_i x_j} \tag{4}$$

in which u_i ($i = 1, 2, 3$) is the velocity components, and p is the fluid pressure. Equation (4) is solved with a finite-difference-based Cartesian grid immersed boundary method [35]. A second-order central difference scheme in space is employed. Time is advanced using a second-order-accurate fractional-step method. This method was successfully applied in many simulations of flapping propulsion [8,24,31,36–39]. More details about the method as well as validations of the fluid solver can be found in our previous work [39–41].

The governing equation of the wing pitching motion is as follows:

$$I_{xx}\ddot{\omega}_x + (I_{zz} - Iyy)\omega_y\omega_z + I_{xy}(\dot{\omega}_x - \omega_x\omega_z) + I_{yz}(\omega_y^2 - \omega_z^2) + I_{xz}(\dot{\omega}_z - \omega_x\omega_y) = M_{\text{aero}} + M_{\text{elastic}} + M_{\text{gravity}} \tag{5}$$

where I_xx, I_yy, I_zz, I_xy, I_xx, and I_xz are elements of the wing's moment of inertia matrix. M_{aero}, M_{elastic}, and M_{gravity} are the torques due to aerodynamic, elastic, and gravitational forces, respectively.

The governing equations of the fluid and the solid (the wing) are strongly coupled via subtime step iterations, which ensure convergence of the wing pitch angle within each time step.

C. Validation

To validate our code, a flapping wing with a torsional axis along the spanwise direction is simulated. The passive pitching of the wing and the flow around this wing is obtained by the aforementioned model. The results are compared with those in Whitney and Wood [13]. The key parameters of the validation case are as follows. The geometry of the wing model as well as its inertial properties are taken from [13]. The flapping amplitude is set to 108 deg, and the flapping frequency is 100 Hz. The natural frequency is $f_n = 233.7$ Hz. We compare the simulated pitching angle of our model with that obtained by Whitney and Wood [13] through both experiments and quasi-steady model calculation in Fig. 2.

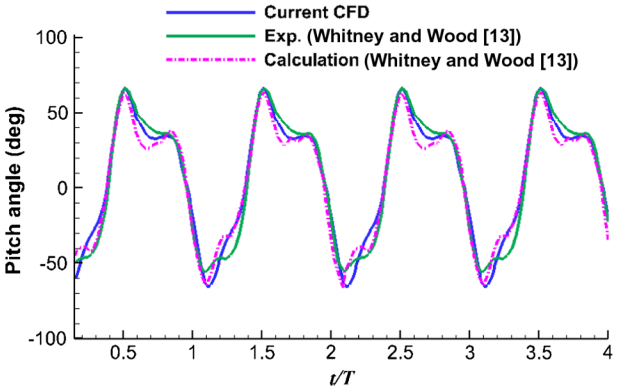

Fig. 2 Comparison of the pitching angle among the current CFD simulation, experimental measurement, and quasi-steady calculation [13].

III. Results

A. Flexible Flapping Wing in Yaw Rotation

We start by keeping nondimensional flexibility of the wing and the mass ratio constant at $Ch = 0.2$ and $M = 1$. When the wing flaps through the air, it pitches about its rotation axis as a result of the combined effects from inertia, aerodynamics, and elastic forces. The elastic force tends to restore the orientation of the wing to its rest orientation at $\eta = 0$, where the wing surface is normal to the flapping direction. The fluid force, on the other hand, tends to orient the wing with the direction of the incoming velocity, where the surface of the wing is parallel to the flapping direction. The net effect of the inertial forces depends on the acceleration of the wing [11,12,18]. The solid black line in Fig. 3 shows the resulting passive wing pitch angle. Note that the pitch angle of the wing is symmetric in DS and US. Next, we impose body rotation and repeat the numerical simulation. Figure 3 shows the passive pitch angle for different normalized body velocities. Notice that the body rotation breaks the DS–US symmetry of the wing pitch angle. This is due to the asymmetric change in the effective Cauchy number of the wing in DS and US (mass ratio remains unchanged). When the body undergoes a yaw rotation, the net incoming velocity to the wing changes, altering the balance between the aerodynamic and elastic torque. In downstroke, the net velocity, and thus the dynamic pressure, increases on the outer wing. The stronger fluid force rotates the wing more toward the incoming velocity direction, which results in decreasing pitch angle (and the geometric angle of attack) of the wing. The opposite occurs in US, where the net velocity, and therefore the dynamic pressure, of the wing decreases. Weakening of the fluid dynamic pressure allows the restoring elastic force to bring the wing orientation closer to its rest orientation (vertical). Consequently, the wing pitch angle increases in US. We will refer to the passive pitch-angle asymmetry as PPA.

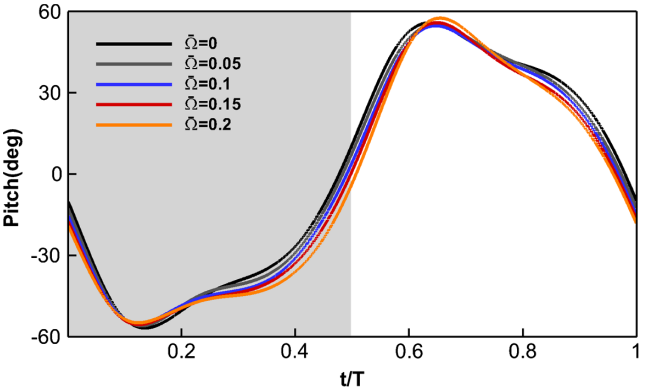

Fig. 3 Time history of the passive pitch angle of the outer wing when the body is in yaw rotation. Different colors represent different $\bar{\Omega}$ values. Duration of downstroke is shaded in gray.

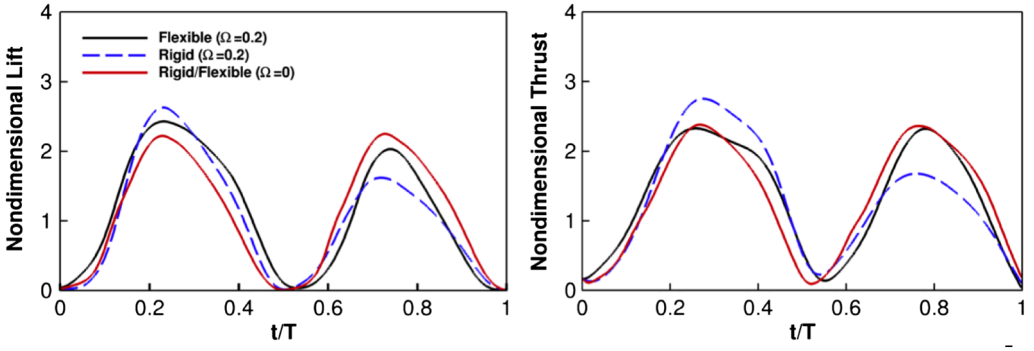

Fig. 4 Time history of nondimensional lift and thrust generated by the outer wing when the body is in yaw rotation of magnitude $\bar{\Omega} = 0.2$. The force is normalized by qbc, where $q = 0.5\rho U^2$.

Figure 4 shows the lift and thrust (nondimensionalized) for the same wing ($Ch = 0.2$ and $M = 1$) as a function of time at $\bar{\Omega} = 0.2$. Similar to the pitch angle, the force generated by the wing is asymmetric in DS and US. For reference, the force generated by the wing at hover is shown by the solid red line. This asymmetry in the force arises from two effects; the first effect is related to the rigid flapping motion of the wing, and the second stems from the passive response of a torsionally flexible flapping wing. The former effect occurs purely due to the asymmetric change in the net incoming velocity to a rigid flapping wing [30] (see dashed blue line in Fig. 4). However, when a flexible wing experiences whole-body rotation, not only the incoming velocity to the wing changes asymmetrically in DS and US but so does the average wing pitch angle. Thus arises the difference in the force asymmetry generated by a flexible versus a rigid wing, which is evident in Fig. 4. Note that the difference in the force generated in DS and US is larger for a rigid wing when compared to a flexible wing.

As was mentioned before (in Sec. II), the difference in the behavior of the outer wing in DS and US can be interpreted as the difference in the behavior of the inner and outer wings during whole-body rotations. Thus, the asymmetry in DS and US behavior of the wing is representative of the asymmetry of the bilateral wings, which can potentially lead to generation of lateral motion. In the following sections, the behavior of the bilateral wings during body yaw rotation will be analyzed based on the simulation of a single wing in the same motion.

B. Effect of Wing Flexibility

Figure 5a shows the difference in the downstroke-averaged geometric angle of attack of the bilateral wings in degrees, $\Delta\alpha = \alpha_i - \alpha_o$, as a function of $\bar{\Omega}$ for different Cauchy number values. The geometric angle of attack is the angle between the wing surface and the wing flapping velocity (stroke plane of the wing). The magnitude of $\Delta\alpha$ is the same in DS and US, but the sign is opposite. In DS, the inner wing has a larger angle of attack, and in US, the outer wing does. The difference in the angle of attack of the bilateral wings increases almost linearly with increase in the body velocity for a constant Cauchy number value. Both the magnitude of $\Delta\alpha$ and its rate of change with rotational velocity is larger for more flexible wings (higher Cauchy number values). At $M = 1$, $\Delta\alpha$ is not a function of Cauchy number for $Ch > 0.2$.

Figures 5b and 5c show ΔC_L and ΔC_T as a function of $\bar{\Omega}$ for different Cauchy number values. $\Delta C_T = C_{T_i} - C_{T_o}$, where subscripts i and o stand for inner and outer wing, respectively. Note that, in the calculation of C_L and C_T, the force is normalized by the net velocity of the wing [Eq. (3)]. This definition is used to separate the effect of the PPA (passive pitch asymmetry, a flexible effect) from that of FCT (flapping counter-torque, a rigid effect) in generating bilateral force asymmetry. For a rigid wing, $C_{T_i} = C_{T_o}$ and $CL_i = C_{L_o}$ because the pitch angles of the bilateral wings are identical. However, that is not the case for a flexible wing. Our results show that both ΔC_L and ΔC_T increase with the body rotational velocity. The variation of ΔC_T with $\bar{\Omega}$ is relatively linear. Both the magnitude of ΔC_T and its rate of change with $\bar{\Omega}$ are larger for lower Cauchy number values. The larger ΔC_T values, however, are an artifact of the higher C_T values for more rigid wings. The smaller the Cauchy number value is, the larger the relative strength of the elastic force is compared to the fluid force. This means that the wing moves with a larger angle of attack through the stroke plane and generates larger thrust/drag force. If we normalize ΔC_T by the average thrust coefficient of the bilateral wings, $\bar{C}_T$, the lines of $\Delta\hat{C}_T = \Delta C_T/\bar{C}_T$ versus $\bar{\Omega}$ collapse close to each other, as shown in Fig. 5d.

Asymmetric change in the bilateral lift and thrust leads to the generation of roll and yaw moments, respectively. The magnitude of the net moment is proportional to the magnitude of asymmetry in the bilateral forces. In the following section, we derive an estimation of the net passive yaw torque generated by a pair of flexible flapping wings, when they are engaged in a whole-body rotation. In addition, we compare and contrast our model against the one derived for a rigid pair of wings in [30]. Although our focus is mainly on the yaw rotation and the passive yaw torque generation in the present paper, it is important to note that the asymmetric changes in the bilateral pitch angles also lead to generation of a net roll moment.

C. Effect of Mass Ratio

To probe how PPA scales with inertial effects, we repeated our simulations for a smaller M value of 0.1. This is closer to the mass ratio observed in aquatic animals. Figure 6 shows $\Delta\alpha$ and ΔC_T as a function of $\bar{\Omega}$. The trends are similar to what was observed for larger mass ratio cases, but the magnitudes of the bilateral wing angle of attack difference and bilateral force coefficient differences are slightly larger for small mass ratio cases. This is not surprising because, at smaller mass ratios, inertial effects are lighter, and thus dynamics of the passive wing pitch is more dominantly governed by the interplay between the fluid and elastic forces.

D. Effect of Passive Pitch-Angle Asymmetry on the Body Motion

To probe how PPA affects the body motion, here we calculate the yaw torque exerted on the body due to the passive asymmetry in the bilateral wing pitch angles. To separate the effect of the passive wing kinematic changes from that of the body rotation only (FCT), we make a comparison between the passive yaw torque generated by a pair of rigid wings versus that generated by a pair of flexible wings.

When a pair of rigid flapping wings is engaged in a whole-body rotation, their net flapping velocity changes asymmetrically. This results in a net passive yaw torque acting on the body whose magnitude is proportional to the rotational velocity of the body. This counteracting torque is referred to as FCT [42]:

$$\tau_r = \frac{1}{2}\rho b^3 c \bar{C}_T l\left[(\omega - \Omega_r)^2 - (\omega + \Omega_r)^2\right] \tag{6}$$

where l is the distance of the center of the action of the force from the body center of mass. Ω_r is the instantaneous yaw velocity of the body.

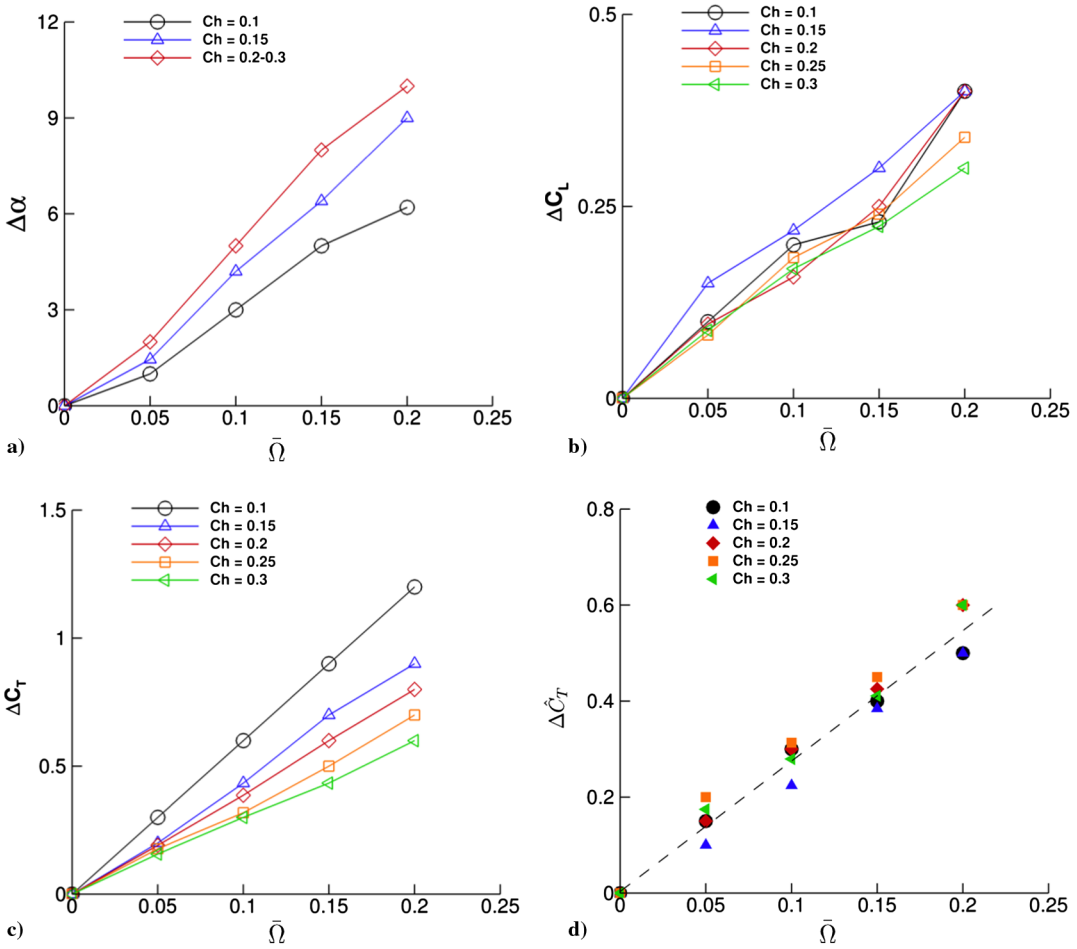

Fig. 5 The difference in the average a) angle of attack (in degrees), b) lift coefficient, c) thrust coefficient, and d) normalized thrust coefficient as a function of $\bar{\Omega}$.

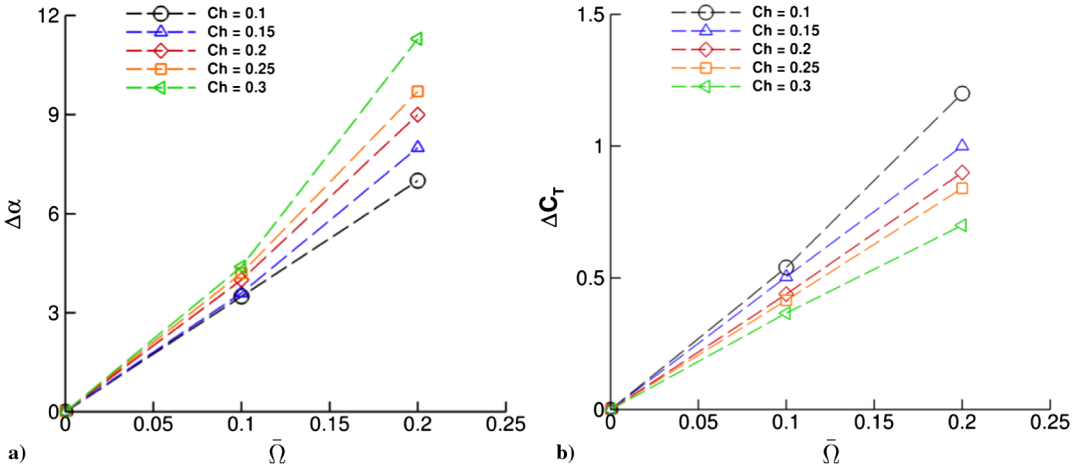

Fig. 6 The difference in the average a) angle of attack, and b) thrust coefficient as a function of $\bar{\Omega}$ for $M = 0.1$.

The subscript r stands for rigid. Note that, for a rigid pair of wings, $\bar{C}_T = C_{T_i} = C_{T_o}$. Equation (6) can be simplified as follows:

$$\tau_r = -4A\omega\Omega_r \tag{7}$$

where $A = (1/2)\rho b^3 c C_T l$. Equation (7) indicates that the passive yaw torque acting on the body (connected to a pair of rigid flapping wings) is proportional to the rotational velocity of the body, or in other words, $\dot{\Omega}_r \propto \Omega_r$. The solution to this simple ordinary differential equation is an exponential function. Thus,

$$\Omega_r = \Omega_0 e^{(-4A\omega/I_b)t} \tag{8}$$

where I_b is the moment of inertia of the whole-body system about the yaw axis of rotation, and Ω_0 is the initial body yaw velocity (at the onset of deceleration phase).

Similar to the case for rigid pair of flapping wings, the net flapping velocities of the bilateral wings are asymmetric for a flexible pair as well. However, for a pair of flexible wings, the thrust coefficients of the bilateral wings are no longer identical. In downstroke, C_T increases on the inner wing, and it decreases on the outer wing.

The thrust coefficient of the inner and outer wing can be expressed as $C_{T_o} = \bar{C}_T - (\Delta C_T/2)$ and $C_{T_i} = \bar{C}_T + (\Delta C_T/2)$, where $\bar{C}_T$ is the average thrust coefficient of the bilateral wings. Thus, the passive yaw torque generated by a pair of flexible wings that are engaged in whole-body rotation can be expressed as follows:

$$\tau_f = \frac{1}{2}\rho b^3 c \bar{C}_T l\left[\left(1+\frac{\Delta\hat{C}_T}{2}\right)(\omega-\Omega_f)^2 - \left(1-\frac{\Delta\hat{C}_T}{2}\right)(\omega+\Omega_f)^2\right] \tag{9}$$

where the subscript f stands for flexible, and $\Delta\hat{C}_T = \Delta C_T/\bar{C}_T$, as was defined in earlier. From the previous section, we know that $\Delta\hat{C}_T$ varies linearly with $\bar{\Omega}$: $\Delta\hat{C}_T = a\bar{\Omega}$. Thus, Eq. (9) can be rewritten as

$$\tau_f = -4A\omega\Omega_f + Aa\Omega_f\omega(1+\bar{\Omega}_f^2) \tag{10}$$

Because $\bar{\Omega}_f^2 \ll 1$,

$$\tau_f \approx -(4-a)A\omega\Omega_f \tag{11}$$

Equation (11) has a form similar to that of Eq. (7) and can be similarly solved for Ω_f:

$$\Omega_f = \Omega_0 e^{(-(4-a)A\omega/I_b)t} \tag{12}$$

Because $a > 0$, the rate of decay in the yaw velocity is always slower for flexible wings. The body yaw velocity half-life of a flexible pair of wings is $4/(4-a)$ times larger than that of a rigid pair.

E. Effect of Body Motion on the Flow Structure of Torsionally Flexible Wings

Here, we compare the flow structure of a flexible versus a rigid flapping wing during whole-body rotation. The nondimensional rotational velocity of the body is set at $\bar{\Omega} = 0.2$. To isolate the effect of the passively induced wing pitch changes, we prescribed the pitch angle of the rigid wing as that of the flexible wing at $\bar{\Omega} = 0$ and $Ch = 0.2$. The Cauchy number for the flexible wing is set to 0.2 as well.

The three-dimensional flow structures of both the rigid and the flexible wing are visualized by plotting the isosurface of the maximal imaginary part of complex eigenvalues of the velocity gradient tensor, $\Lambda_{\max}$, as shown in Fig. 7. Two $\Lambda_{\max}$ values of 40 and 25 are visualized to show the stronger vortex core as well as the weaker surrounding vorticity. Although the major flow structures are similar, differences in vortex evolution and shedding are identifiable. Comparing Figs. 7a–7c and 7d–7f shows that, in downstroke, the leading-edge vortex (LEV) of the rigid wing evolves relatively slower. But more vorticity packs into it, and it eventually grows to become a stronger coherent vortex, which remains attached to the wing at middownstroke. In addition, on the rigid wing, less vorticity is shed out via the tip vortex. The footprint of this is traceable in the plot of force versus time that is shown in Fig. 4. In downstroke, the force peak is larger for the rigid wing, and the peak value is phase-delayed when compared to the peak downstroke force of the flexible wing. Also, the average force generated by the rigid wing in downstroke is larger that of the flexible wing. Note that, in DS, the pitch angle of the outer (flexible) wing decreases (compared to the hovering flight) due to the interplay between the fluid and elastic forces, hence the smaller downstroke force (drag) production when compared to the rigid wing in the same rotational flight.

In upstroke, the story is reversed. Comparing the flow structure of the flexible and rigid flapping wings in Fig. 8 shows that the evolution of the LEV of the flexible wing is delayed when compared to the rigid wing, and the LEV vortex of the flexible wing is stronger at midupstroke. The footage of this is detectable in the plot of the force versus time (Fig. 4), where the peak force (as well as the half-stroke-averaged force) generated by the flexible wing in upstroke is larger than that of the rigid wing, and the phase of the peak force is delayed when compared to the rigid wing. Similar results were found in [42].

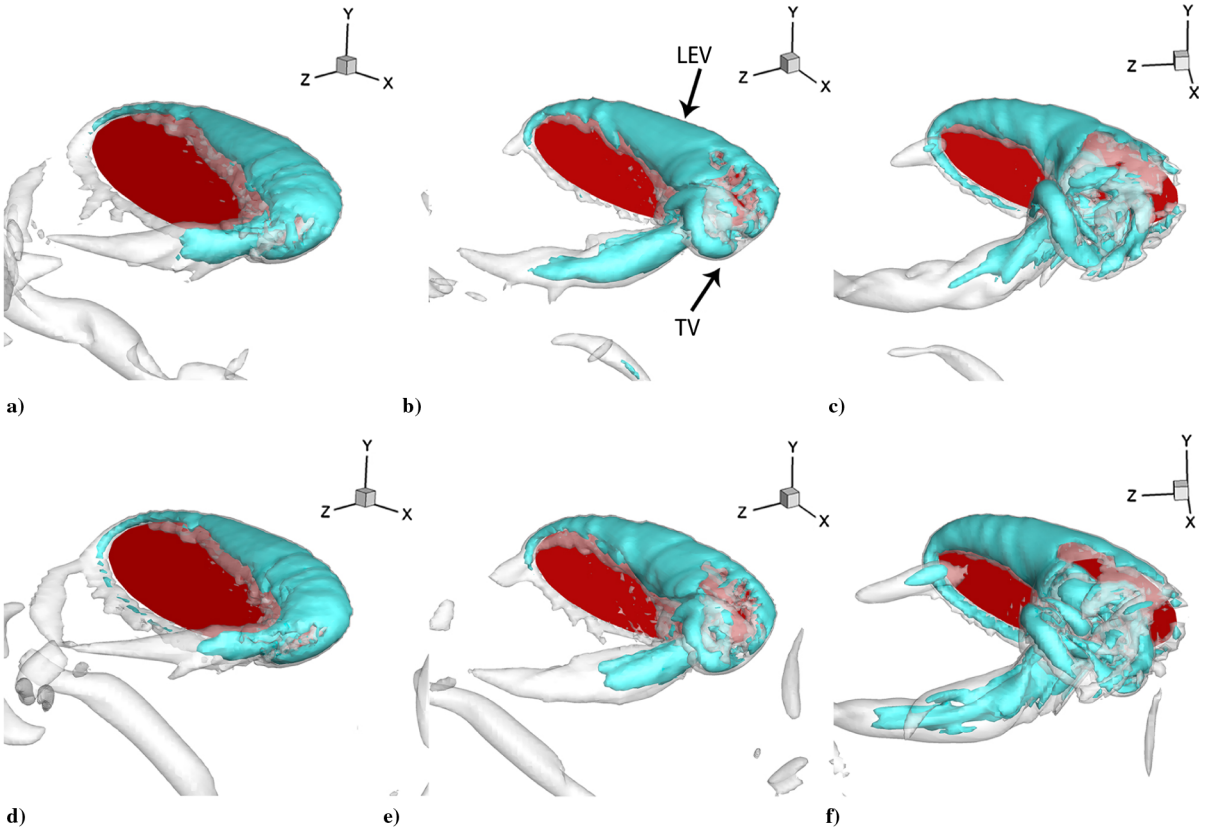

Fig. 7 Visualization of the vortex structure of a torsionally flexible wing at a) $t/T = 0.2$, b) 0.3, c) 0.4, and a rigid wing at d) $t/T = 0.2$, e) 0.3, and f) 0.4.

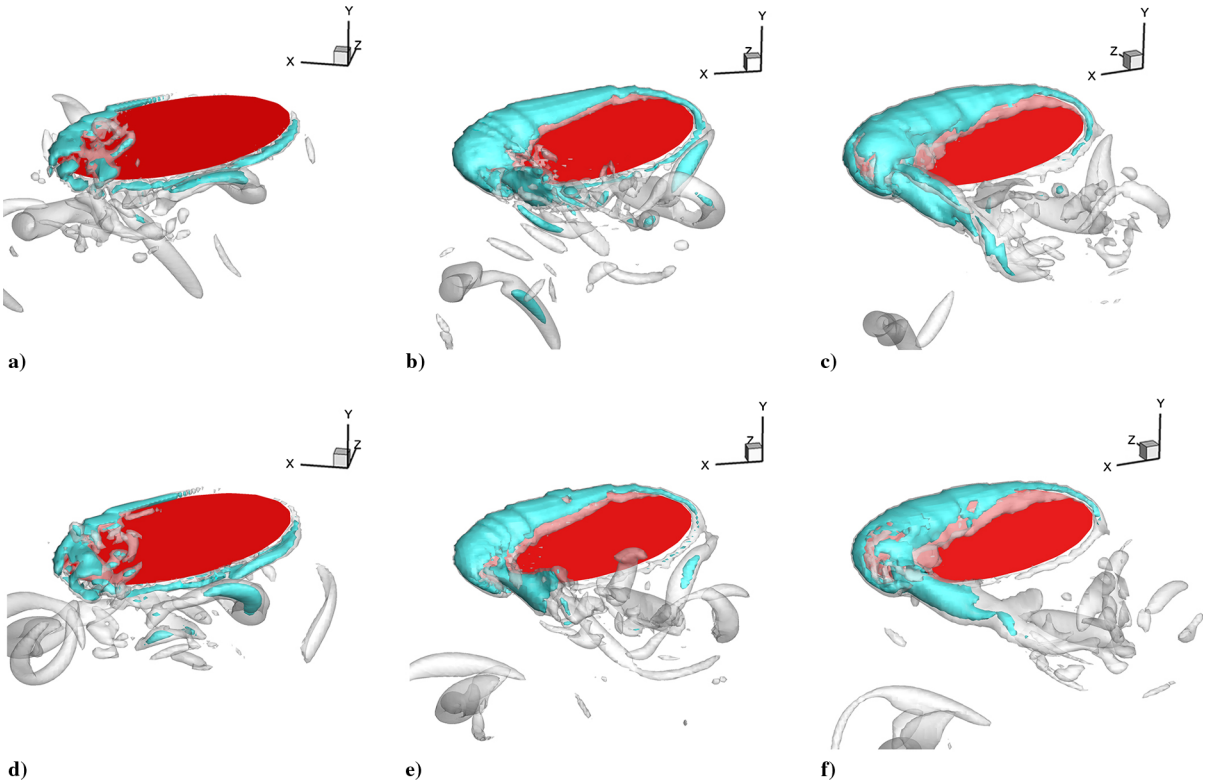

Fig. 8 Visualization of the vortex structure of a torsionally flexible wing at a) $t/T = 0.65$, b) 0.74, c) 0.8, and a rigid wing at d) $t/T = 0.65$, e) 0.74, and f) 0.8.

IV. Conclusions

When flapping through the air, insect wings are subject to aerodynamic and inertial forces that influence their motion and deformation. Through a computational study, which combines a high-fidelity fluid dynamics solver with a torsional spring structure model, we investigated how the wing pitch depends upon the body rotations. Through the present analyses, a passive mechanism has been discovered that allows wing kinematic modulations during the aerial maneuvers that were previously thought to be exclusively active. The passive changes in the wing kinematics act as a complementary mechanism that enhances wing pitch asymmetry during the aerial maneuvers and reduces the damping of the body rotational velocity. Furthermore, it was shown that the present results and conclusions are valid for a large range of wing flexibilities and inertial properties.

To generate in-flight turns, many insects adjust the pitch angle of their bilateral wings [18]. To tune the wing kinematics, they use the flight muscles inside the thorax. Active control of the wing motion requires neural and mechanical feedback from the body motion as well as feedforward motor neurons to transport the control signal to the flight muscle [29]. Therefore, any adjustment in the wing kinematics will cost time and energy. The present analysis indicated that there is an alternative passive pathway by which changes in the flight condition can affect the wing kinematics. Bypassing the active control loop, the passive wing kinematic modulations are fast and energetically efficient. While in rotation, PPA lessens the need for active control. Moreover, because of the reduced damping of the body rotational velocity, an insect with torsionally flexible wings can generate larger turn angles (flight heading change) employing the same amount of initial kinetic energy. In fact, the present experimental measurements on the free-flying damselflies during fast yaw turns (which are published in another document) show that the new model, which includes the effect of wing flexibility, can accurately predict both wing and body kinematics of these insects during the deceleration phase of the maneuver [26,32]. Flapping frequency of damselflies is only about 15–40 Hz, and thus during fast yaw turns, $\bar{\Omega}$ rises up to 0.4 [24,26]. At these large values of $\bar{\Omega}$, the magnitude of passive wing pitch asymmetry is in the order of 10–20 deg. For high-flapping-frequency insects, such as fruit flies and drone flies, $\bar{\Omega}$ is only about 0.05–0.1. According to the present model, at these values of $\bar{\Omega}$, the magnitude of passive wing pitch asymmetry is only about 2–5deg, which is in the same range as the measured wing pitch angle difference during the deceleration phase of aerial turns for these insects [18,43].

Here, the discussion was limited to the deceleration phase of the aerial yaw maneuvers, where the active modulations in the wing kinematics are minimal. Yet these passive changes in the wing kinematics will also occur during the acceleration phase. In the acceleration phase of the maneuver, body rotational velocity, which is initially small, increases wingbeat to wingbeat due to actively induced asymmetries in the motion of the bilateral wings [44]. The asymmetry in the wing kinematics makes the analysis of the passive wing pitch modulations in the acceleration phase relatively more complicated. During this phase, the magnitude of the passive wing pitch asymmetry is determined by the combined effect of the increasing rotational velocity of the body and the asymmetrical flapping velocities. Depending upon the difference in the bilateral wings' net velocities, PPA can either enhance or reduce the aerodynamic torque available for accelerating the body motion. Nevertheless, the present results suggest that the effect of wing flexibility should be considered throughout the whole duration of the aerial maneuvers of flying insects.

The application of the present results is not limited to the maneuvering flight only. The model also suggests that the commonly used assumptions in the analysis of the flight stability and control of the insects should be revisited. Currently, in stability analysis of the insect flight, wing kinematics are assumed to remain unchanged while the motion of the body is perturbed [5,35,45–47]. The present results suggest that this assumption may not always be valid, especially when the ratio of the body's perturbed motion to the wing flapping velocity is large, which occurs at large perturbation values and/or small flapping frequencies.

It is believed that the present results have broad implications in understanding insect flight dynamics, maneuverability, and wing kinematics control. For instance, the present analysis revealed that the motion of a flexible wing is tightly coupled with that of the body

via interactions between the aerodynamic and elastic forces that act on the wing. This connection is missing from the classical model of the insect flight dynamics in which the motion of the body affects that of the wing only through the control signal that is generated after processing the sensory information [29]. On another level, the present results suggest that agile wing kinematic modulations may not necessarily require rapid sensory information. Therefore, a higher level of maneuverability may be achieved employing a simpler sensory and actuation system. The outcomes of our analysis also inform the design of micro air vehicles by unraveling the connection between the wing design and maneuverability of the flight.

Acknowledgments

This work was supported by the National Science Foundation (grant CEBT-1313217) and the U.S. Air Force Research Laboratory (grant FA9550-12-1-007).

References

[1] Combes, S., and Daniel, T., "Flexural Stiffness in Insect Wings 1. Scaling and the Influence of Wing Venation," *Journal of Experimental Biology*, Vol. 206, No. 17, 2003, pp. 2979–2987. doi:10.1242/jeb.00523

[2] Wan, H., Dong, H., and Ren, Y., "Study of Strain Energy in Deformed Insect Wings," *Dynamic Behavior of Materials*, Vol. 1, May 2011, pp. 323–328.

[3] Koehler, C., Liang, Z., Gaston, Z., Wan, H., and Dong, H., "3D Reconstruction and Analysis of Wing Deformation in Free-Flying Dragonflies," *Journal of Experimental Biology*, Vol. 215, No. 17, 2012, pp. 3018–3027. doi:10.1242/jeb.069005

[4] Mountcastle, A. M., and Combes, S. A., "Wing Flexibility Enhances Load-Lifting Capacity in Bumblebees," *Proceedings of the Royal Society B*, Vol. 280, No. 1759, 2013, Paper 20130531.

[5] Zhao, L., Huang, Q., Deng, X., and Sane, S. P., "Aerodynamic Effects of Flexibility in Flapping Wings," *Journal of the Royal Society Interface*, Vol. 7, No. 44, 2010, pp. 485–497. doi:10.1098/rsif.2009.0200

[6] Tanaka, H., Whitney, J. P., and Wood, R. J., "Effect of Flexural and Torsional Wing Flexibility on Lift Generation in Hoverfly Flight," *Integrative and Comparitive Biology*, Vol. 51, No. 1, July 2011, pp. 142–150.

[7] Young, J., Walker, S. M., Bomphrey, R. J., Taylor, G. K., and Thomas, A. L., "Details of Insect Wing Design and Deformation Enhance Aerodynamic Function and Flight Efficiency," *Science*, Vol. 325, No. 5947, 2009, pp. 1549–1552. doi:10.1126/science.1175928

[8] Li, C., Dong, H., and Liu, G., "Effects of a Dynamic Trailing-Edge Flap on the Aerodynamic Performance and Flow Structures in Hovering Flight," *Journal of Fluids and Structures*, Vol. 58, Oct. 2015, pp. 49–65. doi:10.1016/j.jfluidstructs.2015.08.001

[9] Mountcastle, A. M., and Combes, S. A., "Biomechanical Strategies for Mitigating Collision Damage in Insect Wings: Structural Design Versus Embedded Elastic Materials," *Journal of Experimental Biology*, Vol. 217, No. 7, 2014, pp. 1108–1115. doi:10.1242/jeb.092916

[10] Eberle, A., Dickerson, B., Reinhall, P., and Daniel, T., "A New Twist on Gyroscopic Sensing: Body Rotations Lead to Torsion in Flapping, Flexing Insect Wings," *Journal of the Royal Society Interface*, Vol. 12, No. 104, 2015, Paper 20141088. doi:10.1098/rsif.2014.1088

[11] Ennos, A. R., "The Importance of Torsion in the Design of Insect Wings," *Journal of Experimental Biology*, Vol. 140, No. 1, 1988, pp. 137–160.

[12] Ishihara, D., Yamashita, Y., Horie, T., Yoshida, S., and Niho, T., "Passive Maintenance of High Angle of Attack and Its Lift Generation During Flapping Translation in Crane Fly Wing," *Journal of Experimental Biology*, Vol. 212, No. 23, 2009, pp. 3882–3891. doi:10.1242/jeb.030684

[13] Whitney, J. P., and Wood, R. J., "Aeromechanics of Passive Rotation in Flapping Flight," *Journal of Fluid Mechanics*, Vol. 660, Oct. 2010, pp. 197–220. doi:10.1017/S002211201000265X

[14] Walker, S. M., Thomas, A. L., and Taylor, G. K., "Deformable Wing Kinematics in Free-Flying Hoverflies," *Journal of the Royal Society Interface*, Vol. 7, No. 42, 2010, pp. 131–142. doi:10.1098/rsif.2009.0120

[15] Du, G., and Sun, M., "Effects of Unsteady Deformation of Flapping Wing on Its Aerodynamic Forces," *Applied Mathematics and Mechanics*, Vol. 29, No. 6, 2008, pp. 731–743. doi:10.1007/s10483-008-0605-9

[16] Ishihara, D., Horie, T., and Denda, M., "A Two-Dimensional Computational Study on the Fluid–Structure Interaction Cause of Wing Pitch Changes in Dipteran Flapping Flight," *Journal of Experimental Biology*, Vol. 212, No. 1, 2009, pp. 1–10. doi:10.1242/jeb.020404

[17] Beatus, T., and Cohen, I., "Wing-Pitch Modulation in Maneuvering Fruit Flies Is Explained by an Interplay Between Aerodynamics and a Torsional Spring," *Physical Review E*, Vol. 92, No. 2, 2015, Paper 022712. doi:10.1103/PhysRevE.92.022712

[18] Bergou, A. J., Ristroph, L., Guckenheimer, J., Cohen, I., and Wang, Z. J., "Fruit Flies Modulate Passive Wing Pitching to Generate In-Flight Turns," *Physical Review Letters*, Vol. 104, No. 14, 2010, Paper 148101. doi:10.1103/PhysRevLett.104.148101

[19] Wan, H., Dong, H., and Huang, G. P., "Hovering Hinge-Connected Flapping Plate with Passive Deflection," *AIAA Journal*, Vol. 50, No. 9, 2012, pp. 2020–2027. doi:10.2514/1.J051375

[20] Zeyghami, S., Akoz, E., and Moored, K., "Enhancing Propulsive Efficiency Through Proper Design of Bending Patterns of a Flexible Pitching Foil," *Bulletin of the American Physical Society*, Vol. 61, 2016.

[21] Akoz, E., Zeyghami, S., and Moored, K., "Intermittent Swimming with a Flexible Propulsor," *APS Meeting Abstracts*, 2016.

[22] Birch, J. M., Dickson, W. B., and Dickinson, M. H., "Force Production and Flow Structure of the Leading Edge Vortex on Flapping Wings at High and Low Reynolds Numbers," *Journal of Experimental Biology*, Vol. 207, No. 7, 2004, pp. 1063–1072. doi:10.1242/jeb.00848

[23] Dickinson, M. H., Lehmann, F.-O., and Sane, S. P., "Wing Rotation and the Aerodynamic Basis of Insect Flight," *Science*, Vol. 284, No. 5422, 1999, pp. 1954–1960. doi:10.1126/science.284.5422.1954

[24] Bode-Oke, A. T., Zeyghami, S., and Dong, H., "Aerodynamics and Flow Features of a Damselfly in Takeoff Flight," *Bioinspiration & Biomimetics*, Vol. 12, No. 5, 2017, Paper 056006.

[25] Sane, S. P., and Dickinson, M. H., "The Control of Flight Force by a Flapping Wing: Lift and Drag Production," *Journal of Experimental Biology*, Vol. 204, No. 15, 2001, pp. 2607–2626.

[26] Zeyghami, S., and Dong, H., "Coupling of the Wings and the Body Dynamics Enhances Damselfly Maneuverability," arXiv preprint arXiv:1502.06835, 2015.

[27] Alexander, D. E., "Wind Tunnel Studies of Turns by Flying Dragonflies," *Journal of Experimental Biology*, Vol. 122, No. 1, 1986, pp. 81–98.

[28] Zeyghami, S., Babu, N., and Dong, H., "Cicada (Tibicen Linnei) Steers by Force Vectoring," *Theoretical and Applied Mechanics Letters*, Vol. 6, No. 2, 2016, pp. 107–111. doi:10.1016/j.taml.2015.12.006

[29] Dickinson, M. H., Farley, C. T., Full, R. J., Koehl, M., Kram, R., and Lehman, S., "How Animals Move: An Integrative View," *Science*, Vol. 288, No. 5463, 2000, pp. 100–106. doi:10.1126/science.288.5463.100

[30] Hedrick, T. L., Cheng, B., and Deng, X., "Wingbeat Time and the Scaling of Passive Rotational Damping in Flapping Flight," *Science*, Vol. 324, No. 5924, 2009, pp. 252–255. doi:10.1126/science.1168431

[31] Zeyghami, S., Bode-Oke, A. T., and Dong, H., "Quantification of Wing and Body Kinematics in Connection to Torque Generation During Damselfly Yaw Turn," *Science China Physics, Mechanics & Astronomy*, Vol. 60, No. 1, 2017, Paper 014711.

[32] Zeyghami, S., "Wing in the Loop; Integrating the Wing into Dynamics of Insect Flight," Ph.D. Dissertation, Univ. of Virginia, Charlottesville, VA, 2016.

[33] Cheng, B., and Deng, X., "Translational and Rotational Damping of Flapping Flight and Its Dynamics and Stability at Hovering," *IEEE Transactions on Robotics*, Vol. 27, No. 5, 2011, pp. 849–864. doi:10.1109/TRO.2011.2156170

[34] Dai, H., Luo, H., and Doyle, J. F., "Dynamic Pitching of an Elastic Rectangular Wing in Hovering Motion," *Journal of Fluid Mechanics*, Vol. 693, Feb. 2012, pp. 473–499. doi:10.1017/jfm.2011.543

[35] Taylor, G., and Thomas, A., "Animal Flight Dynamics 2. Longitudinal Stability in Flapping Flight," *Journal of Theoretical Biology*, Vol. 214, No. 3, 2002, pp. 351–370. doi:10.1006/jtbi.2001.2470

[36] Liu, G., Dong, H., and Li, C., "Vortex Dynamics and New Lift Enhancement Mechanism of Wing–Body Interaction in Insect Forward Flight," *Journal of Fluid Mechanics*, Vol. 795, May 2016, pp. 634–651. doi:10.1017/jfm.2016.175

[37] Liu, G., Ren, Y., Zhu, J., Bart-Smith, H., and Dong, H., "Thrust Producing Mechanisms in Ray-Inspired Underwater Vehicle Propulsion," *Theoretical and Applied Mechanics Letters*, Vol. 5, No. 1, 2015, pp. 54–57. doi:10.1016/j.taml.2014.12.004

[38] Fish, F. E., Schreiber, C. M., Moored, K. W., Liu, G., Dong, H., and Bart-Smith, H., "Hydrodynamic Performance of Aquatic Flapping: Efficiency of Underwater Flight in the Manta," *Aerospace*, Vol. 3, No. 3, 2016, p. 20. doi:10.3390/aerospace3030020

[39] Wan, H., Dong, H., and Gai, K., "Computational Investigation of Cicada Aerodynamics in Forward Flight," *Journal of the Royal Society Interface*, Vol. 12, No. 102, 2015, Paper 20141116.

[40] Mittal, R., Dong, H., Bozkurttas, M., Najjar, F., Vargas, A., and von Loebbecke, A., "A Versatile Sharp Interface Immersed Boundary Method for Incompressible Flows with Complex Boundaries," *Journal of Computational Physics*, Vol. 227, No. 10, 2008, pp. 4825–4852. doi:10.1016/j.jcp.2008.01.028

[41] Chang, C.-H., Deng, X., and Theofanous, T. G., "Direct Numerical Simulation of Interfacial Instabilities: A Consistent, Conservative, All-Speed, Sharp-Interface Method," *Journal of Computational Physics*, Vol. 242, June 2013, pp. 946–990. doi:10.1016/j.jcp.2013.01.014

[42] Zhong, Q., Liu, G., Ren, Y., and Dong, H., "On the Passive Pitching Mechanism in Turning Flapping Flights Using a Torsional Spring Model," *47th AIAA Fluid Dynamics Conference*, AIAA Paper 2017-3817, 2017.

[43] Zhang, Y., and Sun, M., "Wing Kinematics Measurement and Aerodynamics of Free-Flight Maneuvers in Drone-Flies," *Acta Mechanica Sinica*, Vol. 26, No. 3, 2010, pp. 371–382. doi:10.1007/s10409-010-0339-2

[44] Fry, S. N., Sayaman, R., and Dickinson, M. H., "The Aerodynamics of Free-Flight Maneuvers in Drosophila," *Science*, Vol. 300, No. 5618, 2003, pp. 495–498. doi:10.1126/science.1081944

[45] Xu, N., and Sun, M., "Lateral Dynamic Flight Stability of a Model Bumblebee in Hovering and Forward Flight," *Journal of Theoretical Biology*, Vol. 319, Feb. 2013, pp. 102–115. doi:10.1016/j.jtbi.2012.11.033

[46] Sun, M., and Xiong, Y., "Dynamic Flight Stability of a Hovering Bumblebee," *Journal of Experimental Biology*, Vol. 208, No. 3, 2005, pp. 447–459. doi:10.1242/jeb.01407

[47] Cheng, B., Deng, X., and Hedrick, T. L., "The Mechanics and Control of Pitching Manoeuvres in a Freely Flying Hawkmoth (Manduca Sexta)," *Journal of Experimental Biology*, Vol. 214, No. 24, 2011, pp. 4092–4106. doi:10.1242/jeb.062760

F. N. Coton
Associate Editor